NON-DOUBLE-COUPLE EARTHQUAKES 2. OBSERVATIONS

Angus D. Miller[1] and G. R. Foulger[1]
Department of Geological Sciences
University of Durham
Durham, England, United Kingdom

Bruce R. Julian
U.S. Geological Survey
Menlo Park, California

Abstract. Most studies assume that earthquakes have double-couple (DC) source mechanisms, corresponding to shear motion on planar faults. However, many well-recorded earthquakes have radiation patterns that depart radically from this model, indicating fundamentally different source processes. Seismic waves excited by advective processes, such as landslides and volcanic eruptions, are consistent with net forces rather than DCs. Some volcanic earthquakes also have single-force mechanisms, probably because of advection of magmatic fluids. Other volcanic earthquakes have mechanisms close to compensated linear vector dipoles and may be caused by magmatic intrusions. Shallow earthquakes in volcanic or geothermal areas and mines often have mechanisms with isotropic components, indicating volume changes of either explosive or implosive polarity. Such mechanisms are consistent with failure involving both shear and tensile faulting, which may be facilitated by high-pressure, high-temperature fluids. In mines, tunnels are cavities that may close. Deep-focus earthquakes occur within zones of polymorphic phase transformations in the upper mantle at depths where stick-slip instability cannot occur. Their mechanisms tend to be deviatoric (volume conserving), but non-DC, and their source processes are poorly understood. Automatic global moment tensor services routinely report statistically significant non-DC components for large earthquakes, but detailed reexamination of individual events is required to confirm such results.

1. INTRODUCTION

A large body of evidence connecting earthquakes with faulting comes both from field observations and from the study of seismic waves. In theory, the compressional waves radiated by a shear fault have a four-lobed pattern, with adjacent lobes alternating in polarity. This pattern, and the entire static and dynamic field of a shear fault in an isotropic medium, is identical to that produced in an unfaulted medium by a distribution over the fault surface of pairs of force couples, with each pair arranged so that its net torque vanishes. Seismologists usually specify earthquake mechanisms in terms of equivalent force systems, and shear-fault mechanisms are called "double couples" (DCs).

The hypothesis that earthquake source mechanisms are DCs has become so widely accepted as to have been treated almost as a fundamental law by many seismologists. To a large extent, however, the success of the DC model has been a consequence of limitations in data quantity and quality. Recent improvements in seismological instrumentation and analysis techniques now identify earthquakes whose radiated waves are beyond doubt incompatible with DC force systems and thus with shear faulting. Well-constrained non-DC earthquakes have been observed in many environments, including particularly volcanic and geothermal areas, mines, and deep subduction zones. A companion paper [*Julian et al.*, this issue, hereinafter referred to as paper 1] summarizes seismic source theory and physical processes that might cause non-DC earthquakes. This paper reviews the actual observations. An overview, including references, is given in Table 1, and Figure 1 shows the geographical locations of the most important observations.

2. DESCRIBING NON-DC EARTHQUAKES

Earthquake mechanisms have most often been determined from compressional wave polarities [paper 1, section 3.1], under the assumption that the mechanism is a DC. Polarity observations are plotted on the "focal sphere," an imaginary sphere surrounding the earthquake focus, and orthogonal "nodal" planes are sought that separate compressions and dilatations. For a shear fault, one of these nodal planes represents the fault. The assumptions that the nodal surfaces are planar and mutually orthogonal narrows the range of feasible solutions and makes possible simple graphical methods of data

[1]Also at U.S. Geological Survey, Menlo Park, California.

Reviews of Geophysics, 36, 4 / *November 1998*
pages 551–568
8755-1209/98/98RG-00717*$15.00*
Paper number 98RG00717

TABLE 1. Summary of Observations of Non-Double Couple Earthquakes

Region	Number of Observations: NDC	Number of Observations: Total	Magnitude	Depth, km	Data	Frequency, Hz	Method	Conclusions	Isotropic Component	References
Landslides and Volcanic Eruptions										
Mt. St. Helens, Washington	1	1	M_S 5.2	~0	*P* and *SH* pol, *P*:*S* amp ratio	0.007, 0.05	CSF	two forces, 2 min apart	ND	*Kanamori et al.* [1984]
					L and *R* wf	0.004–0.005	CSF	force	ND	*Kawakatsu* [1989]
Mantaro Valley, Peru	1	1	M_S 7.2	~0	*L* and *R* wf	0.006–0.008	CSF	force	ND	*Kawakatsu* [1989]
Grand Banks, Canada	1	1	M_S 7.2	~0	*P* and *S* pol, *L* and *R* amp	0.025	manual	force	0	*Hasegawa and Kanamori* [1987]
Kalapana, Hawaii	1	1	M_S 7.1	~7	*P* pol, *L* and *R* amp	0.01	manual	force	0	*Eissler and Kanamori* [1987]
					L and *R* wf	0.004–0.005	CSF, CMT	force + DC	~0	*Kawakatsu* [1989]
Long-Period Volcanic Earthquakes										
Izu Ooshima, Japan	1	1	2.5	30	*P* and *S* pol, *S* polarization	~1	manual	oscillating force	ND	*Ukawa and Ohtake* [1987]
Sakurajima, Japan	19	21	M_W 2–3	0–4	*P* pol and amp, *S* polarization	~1	LSQ	vertical dipole	±	*Iguchi* [1994]
Sakurajima, Japan	2	2	M_W 2.5–3	0–4	*P* and *S* waves	~0.1	LSQ	$M_{xx} \approx M_{yy} \approx 2M_{zz}$ + weak vertical force	−	*Uhira and Takeo* [1994]
Short-Period Volcanic and Geothermal Earthquakes										
Bardarbunga, Iceland	7	7	5.2–5.6	shallow	wf	~0.02	CMT	$0.36 < \varepsilon < 0.48$ Ring fault?	ND	*Ekström* [1994a]
Reykjanes Peninsula, Iceland	6	433	M_{IL} 0–4.4	1–7	*P* pol	~10	manual	not DC	ND	*Klein et al.* [1977]
Hengill, Iceland	56	131	M_{IL} −2.0 to 2.2	2–7	*P* pol	~10	manual	not DC	+	*Foulger and Long* [1984], *Foulger* [1988b], *Foulger and Julian* [1993]
Hengill, Iceland	81	98	$M_W < 1.5$	2–8	*P* and *S* pol, amp ratios	~5	LP	$-0.4 < \varepsilon < 0.3$	+	Miller [1996], *Julian et al.* [1997]
Krafla, Iceland	5	153	$M_{IL} < 2.1$	0–3	*P* pol.	~10	manual	not DC	±	*Arnott and Foulger* [1994a, b]
Miyakejima, Japan	31	31	$M_{IL} \sim 1.2$–2.2	1–5	*P* and *S* amp *P*:*SV* amp ratios	~10	LSQ	tensile + shear fault?	±	*Shimizu et al.* [1987]
Mt. Unzen, Japan	1	1	M_{JM} 3.2	10	*P* pol *P*:*SV* amp ratios	~10	LSQ	tensile + shear fault?	+	*Shimizu et al.* [1988]
Long Valley caldera, Calif.	3	4	$M_L \sim 6$	7–10	*P* and *SH* pol *P* and *SH* wf *L* and *R* amp and phs	0.02–10	LP, CMT, LSQ	$\varepsilon = 0.3$–0.4 time-invariant mechanisms	~0	*Ekström and Dziewonski* [1983], *Barker and Langston* [1983], *Julian* [1983], *Julian and Sipkin* [1985]
Tori Shima, Japan	1	1	M_S 5.5	10	*P* and *SH* wf *L* and *R* amp and phs	0.004–0.1	Various	~CLVD intrusion?	+?	*Kanamori et al.* [1993]
Earthquakes at Mines										
URL, Manitoba	18	33	M_W −4 to −2	0.42	*P* pol, amp	>1000	LSQ	tensile failure	±	*Feignier and Young* [1992]
Witwatersrand, South Africa	7	10	M_W 1.9–3.3	1.9–3.3	NF amp	2–10	LSQ	implosive	−	*McGarr* [1992a, b]
Coeur d'Alene, Idaho	>10	21	−1.7 to 1.3	1.3–3.4	*P* pol	~10	manual	implosive	−	*Stickney and Sprenke* [1993]
Deep Focus Earthquakes										
Subduction zones	?	?	$M_W < 8.5$	300–700	*L* and *R* wf *P* and *S* wf	0.003–0.40	CMT	ε often <0	~0	*Kuge and Kawakatsu* [1993]
Other										
Philippine Sea	1	1	M_W 4.6	57	*P* pol	0.003–0.01	manual	phase transformation	−	*Hurukawa and Imoto* [1993]
Guerrero, Mexico			3.0–6.9	0–50	*P* and *S* spectral ratios	10–50	manual	fault-normal motion	?	*Castro et al.* [1991]

Notation and abbreviations are as follows: (magnitude) M_W, moment magnitude; M_L, local magnitude; M_{IL}, Iceland local magnitude; M_{JM}, Japan local magnitude; m_b, body wave magnitude; M_S, surface wave magnitude; (data) *P*, compressional waves; *S*, shear waves; *SH*, horizontally polarized shear waves; *L*, Love waves; *R*, Rayleigh waves; NF, near-field waves; wf, waveforms; pol, polarities; amp, amplitudes; phs, spectral phase; (method) CSF, centroid single-force inversion; CMT, centroid moment tensor inversion; LSQ, least squares; LP, linear programming; manual, trial-and-error forward modeling; (Isotropic component) +, explosive; −, implosive; ND, not determined.

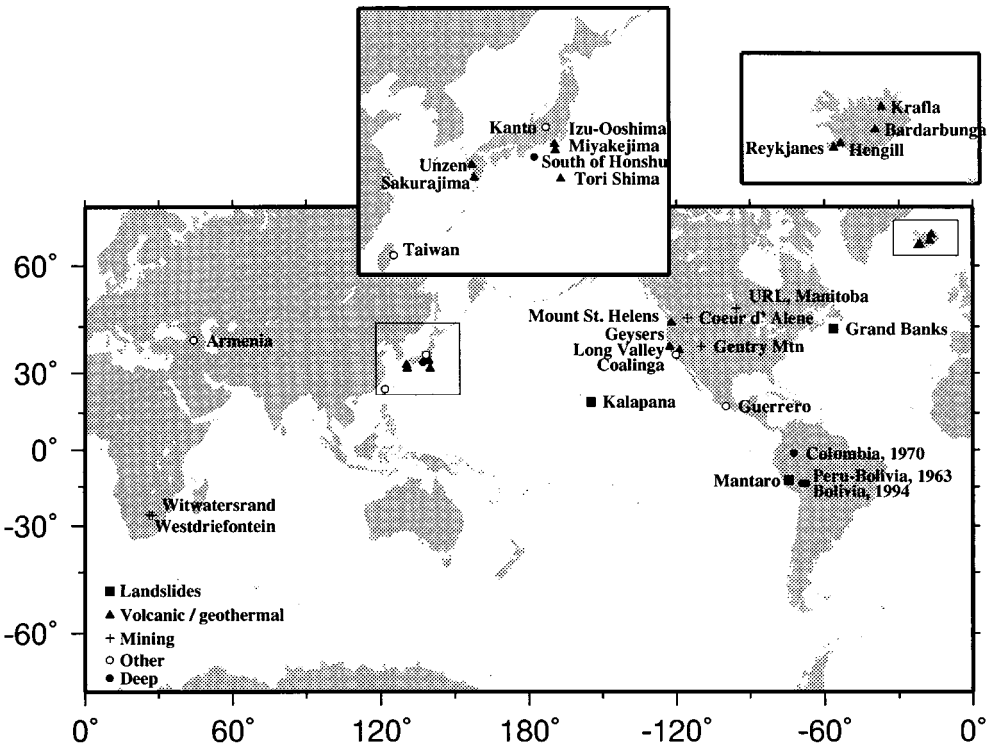

Figure 1. Map showing locations of earthquakes discussed in this paper. Boxes show locations of inset maps of Japan and Iceland.

interpretation. For general non-DC sources, however, the nodal surfaces are not necessarily planes, the range of possible interpretations is much wider, and graphical solution is impractical.

To surmount this problem, and to resolve general non-DC source mechanisms, it is almost always necessary to use data other than just *P* wave polarities, such as wave amplitudes or waveforms. Virtually any kind of seismic wave may be used and many analysis methods have been devised [paper 1, sections 3.3–3.5]. Notable among these are methods that invert amplitude ratios, to reduce distortion by structural complexity [paper 1, section 3.4], and waveform inversion methods [paper 1, section 3.5], which can determine temporal variations in the source mechanism.

Non-DC source mechanisms are almost always expressed as symmetric moment tensors, which require decomposition of some kind to facilitate comprehension [paper 1, section 2.6]. We divide a moment tensor into a volumetric and a deviatoric part [paper 1, equation (16)] and describe the departure of the deviatoric part from a DC by the parameter $\varepsilon = -M'_1/|M'_3|$, where M'_1 and M'_3 are the absolutely smallest and largest deviatoric principal moments. The parameter ε is zero for a DC, and ± 0.5 for a "compensated linear vector dipole" (CLVD). Figure 2 shows decompositions of the most important mechanisms discussed in this paper.

The equivalent force system of an earthquake does not uniquely identify the physical source process. The force system is a phenomenological description of the source and is all that can be determined from seismological observations, but different physical interpretations are generally possible. For example, a DC could correspond to shear slip on a planar fault or on an orthogonal "conjugate" fault, or to opening of a tensile crack and simultaneous closing of an orthogonal crack, or to many other things. To understand earthquake processes, therefore, we must appeal to nonseismological disciplines such as geology and rock physics.

3. OBSERVATIONS OF NON-DC EARTHQUAKES

3.1. Landslides and Volcanic Eruptions

Landslides and volcanic eruptions have equivalent force systems that in theory include net forces [paper 1, section 4.1]. Landslide mechanisms should also include net gravitational torques (asymmetric moment tensors) [paper 1, section 4.1.2], but such models have not yet been applied to seismic data. Several sources of these types have been observed seismically.

The Mount St. Helens, Washington, eruption of May 18, 1980, began with a landslide with a mass of about 5×10^{13} kg that traveled about 10 km northward from the volcano. The identical polarities of *P* waves at some Global Digital Seismograph Network (GDSN) stations, along with large *P*:*S* amplitude ratios, rule out a DC mechanism but can be explained by two forces, a near-horizontal, southward directed force representing the landslide [*Kanamori and Given*, 1982; *Kanamori et al.*, 1984; *Kawakatsu*, 1989] and a vertical force representing the eruption (Figure 3) [*Kanamori et al.*, 1984].

One of the largest landslides in history occurred in the Mantaro Valley, Peru, on 26 April 1974. This rock-

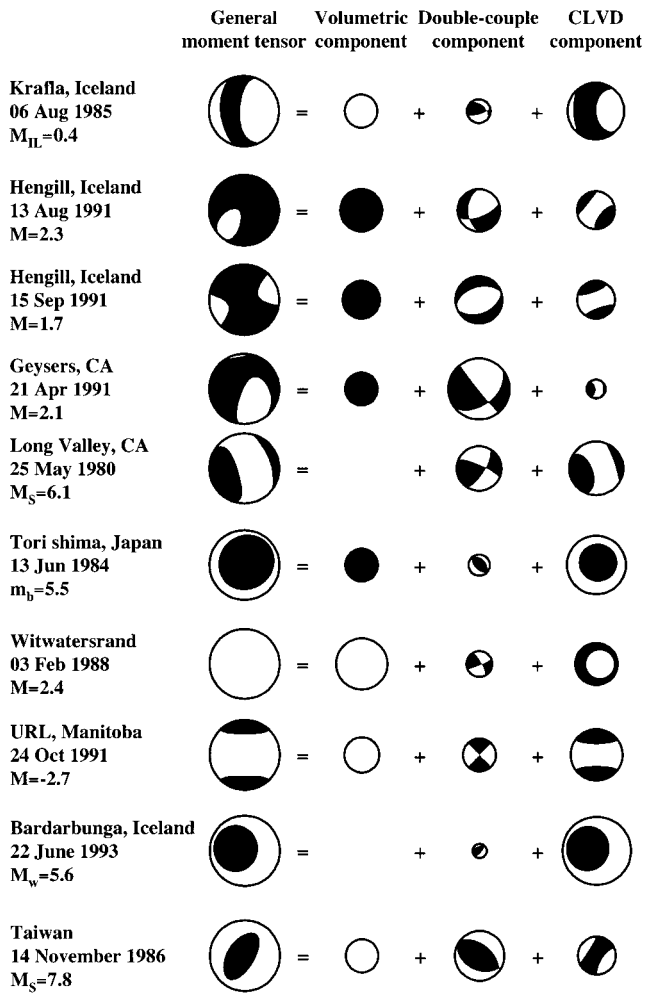

Figure 2. Decompositions of the moment tensors of some of the earthquakes discussed in this paper. The *P* wave polarity distributions for the complete moment tensors and for their volumetric, double-couple (DC), and compensated linear vector dipole (CLVD) components are shown in lower focal hemisphere equal area projection. Areas of circles are proportional to relative seismic moments. The Underground Research Laboratory (URL), Manitoba, earthquake has an arbitrary orientation.

slide avalanche had a volume of about 10^9 m^3, measured more than 8 km along its longest side, and its centroid traveled 4 to 6 km. It excited long-period seismic waves that were recorded at seven digital long-period instruments at teleseismic distances [*Kawakatsu*, 1989]. A "centroid single force" (CSF) inversion, analagous to centroid moment tensor inversion [paper 1, section 2.3.3], of long-period seismic waves with frequencies between 6 and 8 mHz (periods of 167–125 s) yielded a near-horizontal force oriented SW, a direction consistent with that of the slide.

The M_S 7.2, November 18, 1929, Grand Banks, Canada, earthquake generated a submarine turbidity current that traveled 1700 km and severed 12 trans-Atlantic undersea cables [*Doxsee*, 1948; *Hasegawa and Kanamori*, 1987]. Available seismic data consist of *P* and *S* wave polarities and surface wave amplitude spectra from 50 global seismic stations of widely varying instrumental response. These observations are consistent with a northward directed horizontal force, and thus with a southward landslide.

The M_S 7.1 Kalapana earthquake of November 29, 1975, on the island of Hawaii accompanied large-scale subsidence along a 50-km zone on the southwest flank of Kilauea volcano, with a maximum coseismic displacement of 3 m vertically and 8 m horizontally. A 15-m tsunami on nearby beaches indicates that substantial vertical motion occurred on the seafloor also. Initial DC interpretations of observed *P* wave polarities involved shear slip on a near-horizontal fault [*Ando*, 1979], but such a mechanism is inconsistent with the Love wave radiation pattern. An alternative shear model involves slip on a near-horizontal fault and on multiple planes of different orientations. *Eissler and Kanamori* [1987] showed that a single force of about 1.6×10^{15} N in the direction opposite to the observed horizontal motion fits the observed Love wave amplitudes much better than does the DC model of *Ando* [1979] and also is consistent with observed *P* wave polarities. CSF [*Kawakatsu*, 1989] and Harvard centroid moment tensor (CMT) inversions yield combinations of a horizontal force and a DC on a nearly horizontal plane. The source mechanism of the Kalapana earthquake thus remains ambiguous.

3.2. Long-Period Volcanic Earthquakes

"Long-period" volcanic earthquakes have dominant frequencies an order of magnitude lower than those of most earthquakes with comparable magnitudes [e.g., *Hasegawa et al.*, 1991]. Because of their close association with volcanic tremor, they are attributed to unsteady flow of magmatic fluids and are expected to have mechanisms involving net forces [paper 1, section 4.1.4]. The mechanisms of long-period earthquakes may, in the future, provide estimates of flow rates, viscosities, etc., of flowing magma, which would be of obvious value in monitoring volcanoes.

Ukawa and Ohtake [1987] performed one of the few studies that allowed for net forces, of a 33-km-deep, long-period earthquake that preceeded by about a year the 1986 eruption of Izu Ooshima volcano, Japan. The seismograms are characterized by nearly monochromatic *S* wave trains with dominant frequencies of about 1 Hz, lasting for more than a minute (Figure 4). The *P*:*S* amplitude ratios are small and are inconsistent with sources involving tensile cracks or resonance of magma bodies. The *S* wave polarization directions are, however, consistent with a force oriented north-south.

Several types of non-DC earthquakes occur at the intensively monitored Sakurajima volcano in southern Kyushu, Japan. This volcano is continuously active, with frequent eruptions and earthquakes [*Iguchi*, 1994], and is monitored by a high-quality local network with eight seismographs, six of which have three components, as well as tiltmeters, extensometers, acoustic sensors, and

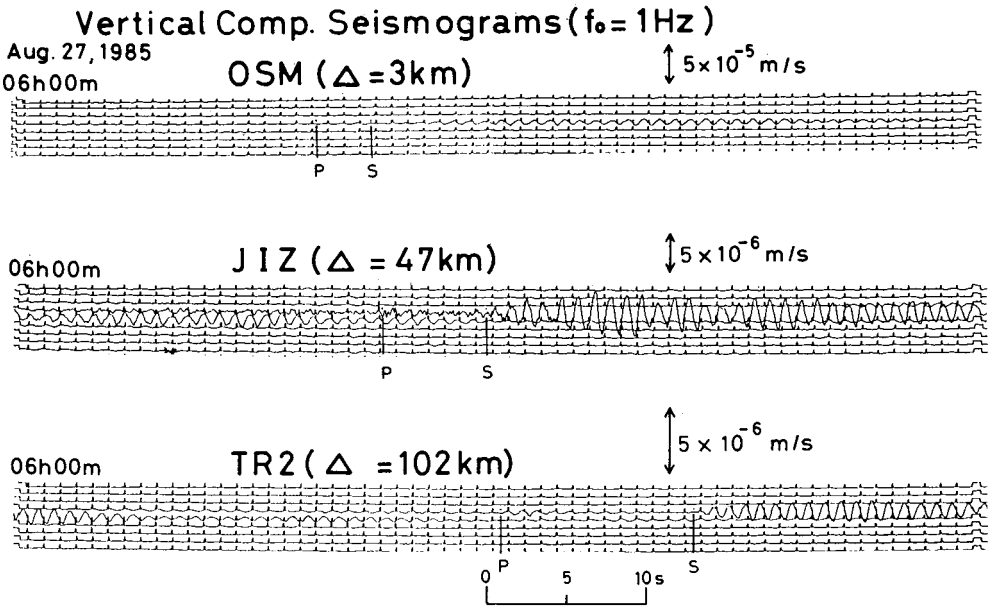

Figure 4. Examples of vertical component seismograms from the long-period earthquake of August 27, 1985, beneath Izu Ooshima volcano, Japan. Note nearly sinusoidal wave trains of long duration. From *Ukawa and Ohtake* [1987, Figure 2].

video cameras. Low-frequency "BL-type" earthquakes occur in swarms when the volcano is active: "BH-type" events are deeper, excite higher-frequency waves, and tend to occur when the volcano has been dormant for a few months; and "explosion" earthquakes accompany crater eruptions that radiate spectacular visible shock waves into the atmosphere [*Ishihara*, 1985]. BH-type and explosion earthquakes have entirely compressional *P* wave polarities, whereas BL-type earthquakes have either entirely compressional or entirely dilatational polarities. *S* waves from all three types of earthquakes are vertically polarized.

Uhira and Takeo [1994] studied two explosion earthquakes, inverting three-component waveforms from three local stations. The derived moment tensor time functions for one earthquake are consistent with deflation of a north striking vertical crack [paper 1, section 2.4.3]. The other earthquake is similar except that the M_{xx} and M_{yy} components are about equal, indicating a source with azimuthal symmetry. Rapid deflation of vertical cracks might rapidly expel gas into the atmosphere and excite the shock waves that accompany explosion earthquakes. Vertical forces accompanying the earthquakes, which are expected consequences of eruption [paper 1, section 4.1.3] are consistent with the observations but are not resolved well. *Iguchi* [1994] inverted *P* wave amplitudes for several BH, BL, and explosion earthquakes to obtain "moment acceleration" ($\dot{\mathbf{M}}$) tensors. The results differ from those of *Uhira and Takeo* [1994] and suggest that all the earthquakes are dominated by vertical dipole components, as would happen for opening of horizontal cracks. The discrepancies between the results of these two studies may reflect the difficulty of resolving between vertical forces and vertical dipoles.

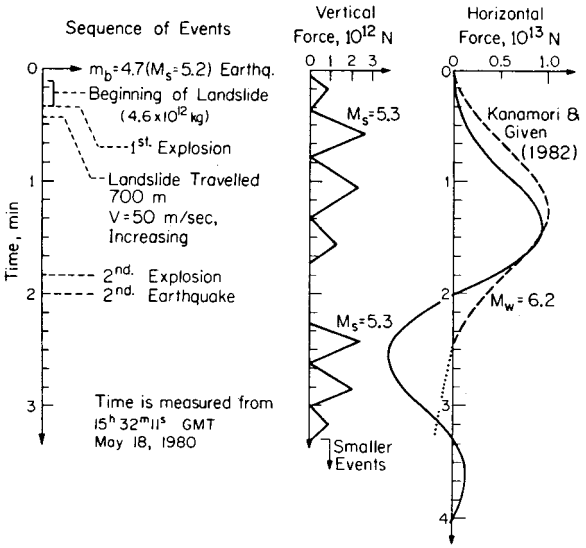

Figure 3. Equivalent force model of the May 18, 1980, eruption of Mount St. Helens, Washington, derived from seismic wave observations. (left) Time line showing the sequence of events reconstructed from photographic and other observations. (middle) Vertical force caused mainly by the eruption, which consists of two major pulses, each composed of subevents. Positive values indicate downward force. (right) Horizontal force caused mainly by the landslide. Positive (southward) forces indicate acceleration of the slide, and negative values indicate deceleration. From *Kanamori et al.* [1984, Figure 16].

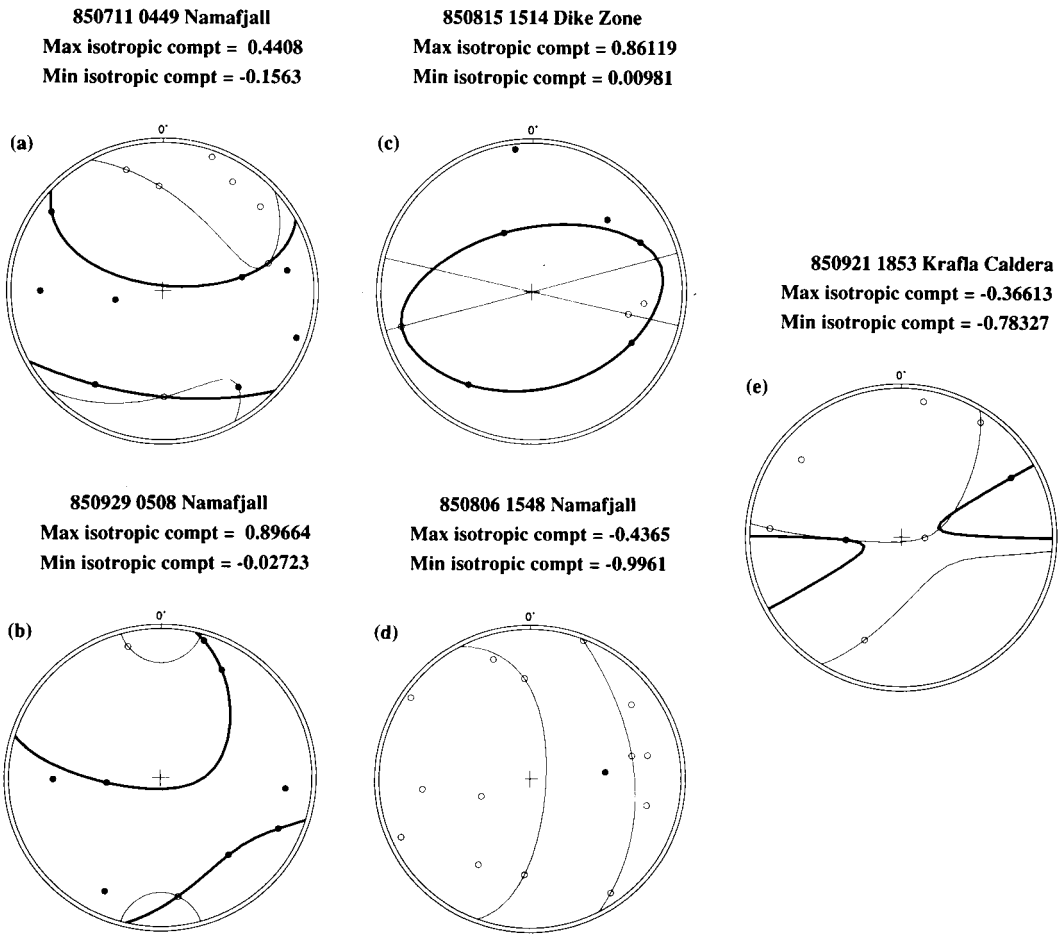

Figure 5. *P*-wave polarities for non-DC earthquakes at the Krafla geothermal area, Iceland. Positions of rays were computed by ray tracing in a three-dimensional crustal model. Thin lines indicate compressional wave nodes of the most explosive possible mechanisms; thick lines show nodes of the most implosive mechanisms. The event shown in Figure 5d has only one compressive arrival, so the compressional field of the most implosive solution is vanishingly small. The origin dates and times are indicated, along with the relative moments of the extreme isotropic components. After *Arnott and Foulger* [1994b].

3.3. Short-Period Volcanic and Geothermal Earthquakes

Observations, many from dense, local seismic networks giving good focal sphere coverage, show that earthquakes in several volcanic areas have non-DC mechanisms. The data in many cases have been subjected to careful analysis, including waveform modeling [e.g., *Julian and Sipkin*, 1985], corrections for wave propagation through heterogeneous structures determined from tomography [e.g., *Arnott and Foulger*, 1994b; *Ross et al*., 1996; *Miller et al*., 1997; *Julian et al*., 1996b], and use of multiple phases in determining moment tensors [paper 1, section 3.4] [e.g., *Julian and Foulger*, 1996]. The clearest cases are from Iceland, California, and Japan.

Three volcano-geothermal areas on the spreading plate boundary in Iceland, on the Reykjanes Peninsula, at the Hengill-Grensdalur triple junction, and at the Krafla volcanic system, have been studied with dense temporary seismometer networks. At all three areas, small earthquakes were found that have unequal dilatational and compressional areas on the focal sphere, suggestive of isotropic components in their mechanisms. In all three regions, anomalous earthquakes were intermingled spatially with DC events, suggesting that the non-DC mechanisms probably are not artifacts of instrumental errors or propagation through heterogeneous structure.

The studies at Reykjanes [*Klein et al*., 1977] and Krafla [*Arnott and Foulger*, 1994a, b] used networks of 20–30 vertical-component sensors with analog recording. From Reykjanes, only a few non-DC mechanisms were found out of several hundred determined. For these, most *P* wave polarities were compressional, suggesting volume increases at the sources. Five non-DC events were identified at Krafla, of which two indicated expansion, two indicated contraction, and one had no resolvable isotropic component (Figure 5). An 1981 study at the Hengill-Grensdalur triple junction [*Foulger and Long*, 1984; *Foulger*, 1988a; *Foulger et al*., 1989] using 23 vertical-component sensors and analog record-

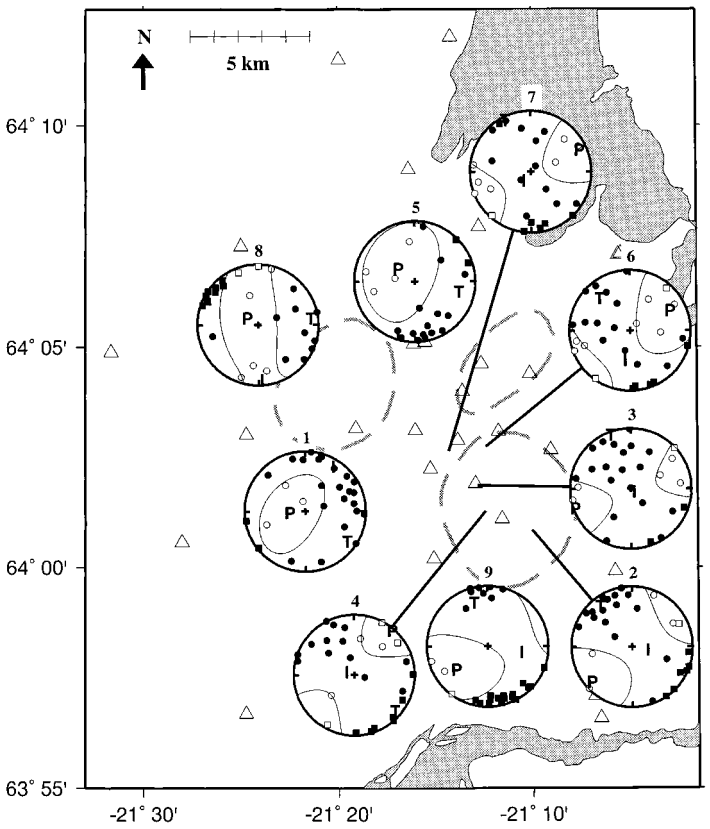

Figure 6. Map of the Hengill-Grensdalur volcanic complex, SW Iceland, showing focal mechanisms of nine representative earthquakes. Events 5, 6, 8, and 9 are interpreted as DCs. *P* wave polarities (solid circles indicate compressions; open circles indicate dilatations) and *P* wave nodes are shown in upper focal hemisphere equal area projection. Squares denote downgoing rays plotted on the upper hemisphere. *T*, *I*, *P* are positions of principal axes. Lines indicate epicentral locations. Where lines are absent, mechanisms are centered on epicenters. Triangles indicate seismometer locations; dashed lines show outlines of main volcanic centers. From *Miller* [1996].

ing found an unusually high percentage of non-DC mechanisms. Presently, Hengill-Grensdalur is the richest source of non-DC earthquakes known. A second experiment in 1991, using 30 three-component sensors and digital recording (Figure 6) [*Miller*, 1996; *Julian et al.*, 1997], showed that about 70% of 98 carefully studied events involved expansion, while only one involved contraction. The deviatoric components were highly variable, with ε values spread over practically the entire possible range.

The persistent small-magnitude earthquake activity at some geothermal areas in Iceland, such as Hengill-Grensdalur, may be caused by thermal contraction in the geothermal heat sources (Figure 7) [*Foulger and Long*, 1984]. The tensile stress fields caused by contraction would favor crack opening, which gives expansional

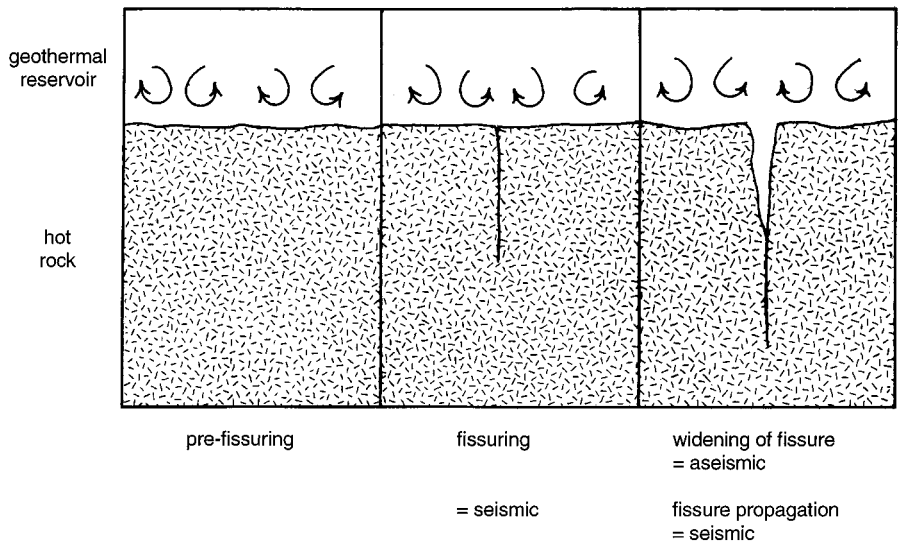

Figure 7. Schematic illustration of the process of seismogenic tensile cracking by thermal stresses caused by convective cooling of rocks at the heat source of a geothermal system. From *Foulger* [1988b].

mechanisms such as are observed. Thermal contraction cannot, however, explain the rarer contractional earthquakes, nor can it explain why, for both types of events, *P* wave polarities are usually mixed. Mixed polarities require some process in addition to crack opening or closing, such as fluid flow [paper 1, section 4.3.3] or shear faulting [*Miller*, 1996], which might also explain (stick-slip instability) how crack closing could be sudden [paper 1, section 4.3.5]. However, at least at Hengill-Grensdalur, observed ε values for many events lie well outside the range for mixed tensile and shear faulting.

It is not known whether non-DC earthquakes like those in Iceland occur along submarine parts of the mid-ocean ridge (MOR) system. The recent discovery of large geothermal areas associated with "black smokers" along spreading ridges tends to support this notion. Unfortunately, deploying ocean bottom seismometers is difficult and expensive, so high-quality observations of small MOR earthquakes are rare. A few observations of MOR microearthquakes exist that are compatible with DC mechanisms only if dilatational polarities are assumed for large areas of the focal sphere devoid of data [e.g., *Toomey et al*., 1985, 1988].

Non-DC geothermal earthquakes are not confined to spreading plate boundaries. Events with volumetric mechanisms occur at The Geysers steam field, in the coast ranges of northern California [*Ross et al*., 1996]. Industrial steam extraction and water reinjection there induces thousands of small earthquakes per month, mostly within the reservoir. The mechanisms are typically closer to DCs than those of Icelandic geothermal earthquakes, and non-DC components are not usually detectable from *P* wave polarities alone but can be resolved using amplitude ratios. As in Iceland, most non-DC events are explosive but have mixed *P* wave polarities (Figure 8), and some might be caused by simultaneous tensile cracking and shear faulting [paper 1, section 4.3.5].

Earthquakes with similar radiation patterns, some of them moderately large, accompany magmatic and volcanic activity, most notably in Japan and California. Many non-DC earthquakes with *P* wave polarities that are either all dilatational or all compressional accompanied the 1983 eruption of Miyakejima volcano, in the Izu island arc south of Honshu, Japan (Figures 9a, and 9b) [*Shimizu et al*., 1987; *Ueki et al*., 1984]. The earthquakes radiated significant *S* waves, so their mechanisms were not purely isotropic. The *P* wave polarities and *P* and *SV* wave amplitudes are compatible with combined tensile and shear faulting [paper 1, section 4.3.5]. Such an interpretation is supported by the observation that many open cracks formed prior to the eruption. A similar but substantially larger earthquake, of magnitude 3.2, occurred 10 km beneath the Unzen volcanic region, in western Kyushu, in 1987 (Figure 9c) [*Shimizu et al*., 1988; H. Shimizu, personal communication, 1988]. The tensile-shear fault model proposed for the Miyakejima earthquakes also fits the polarities and $P:SV$ amplitude ratios of this earthquake, with the tensile fault striking east-west, parallel to the Unzen graben.

Long Valley caldera, in eastern California, has experienced some of the largest clearly non-DC earthquakes. Four earthquakes with $M_L > 6$ occurred there in May 1980 (Figure 10), and at least two of them had non-DC mechanisms. These events followed 2 years of unrest, characterized by increasing seismicity and surface deformation indicating magma chamber inflation [*Rundle and Hill*, 1988]. Unusually complete data are available, including polarities of short- and long-period *P* waves, long-period *P* waveforms, and surface wave amplitudes and initial phases. Moment tensor inversions of different subsets of the data, conducted independently and using different methods [*Given et al*., 1982; *Barker and Langston*, 1983; *Julian*, 1983; *Ekström and Dziewonski*, 1983, 1985; *Julian and Sipkin*, 1985], all give similar nearly CLVD mechanisms for the largest and best recorded event. The fourth earthquake, about 13 km away, had a similar non-DC mechanism, which suggests that the non-DC components are not artifacts of wave propagation effects.

Any volumetric components in the Long Valley earthquakes are unresolvably small, so it is possible that the events involve complex shear faulting [paper 1, section 4.2]. This hypothesis is not supported, however, by the finding of *Julian and Sipkin* [1985] that the largest event consists of three subevents with similar non-DC mechanisms. Tensile faulting at high fluid pressure, perhaps associated with dike intrusion, has also been suggested [*Julian*, 1983; *Aki*, 1984; *Julian and Sipkin*, 1985]. In that case, the volumetric component expected for a tensile fault [paper 1, section 4.3.1] must be compensated by some other process, such as fluid flow.

A M_S 5.6 earthquake similar in mechanism to the Long Valley earthquakes, though differently orientated, occurred near Tori Shima island, in the Izu-Bonin arc, on June 13, 1984. It generated tsunamis much larger than expected for its magnitude [*Satake and Kanamori*, 1991] and had anomalous seismic radiation, nearly lacking horizontally polarized shear (*SH*) and Love waves and with little azimuthal variation in amplitudes or waveforms of other phases. All *P* wave first motions were compressional. These observations indicate a source approximately symmetrical about a vertical axis and rule out DC mechanisms. *Kanamori et al*. [1993] inverted surface and body waves and obtained moment tensors with ε values between 0.3 and 0.4. Because the earthquake was shallow, its full moment tensor cannot be determined well [paper 1, section 3.6.3], but the data are consistent with a mechanism close to a CLVD having a vertical symmetry axis (Figure 2). Intrusion of a laccolith into ocean floor sediments would posses the required symmetry, and the resulting uplift of the ocean floor might explain the large tsunami. The seismic moment and source duration require intrusion of approximately 0.02 km^3 within 10–40 s, a rate that *Kanamori et al*. [1993] reckoned may be possible for a mixture of

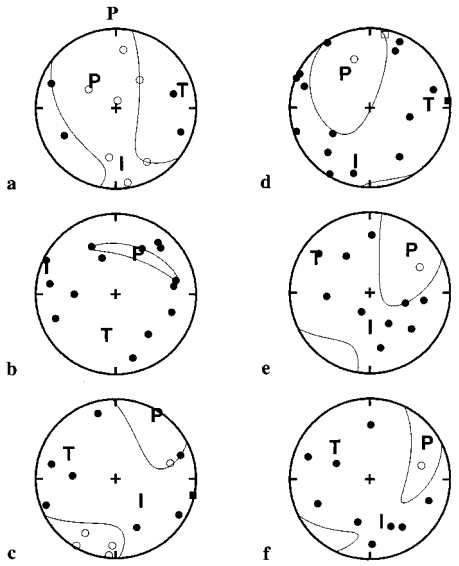

Figure 8. Focal mechanisms of six well-constrained earthquakes at The Geysers geothermal area, California, obtained from inversion of *P* wave polarities and *P*:*SH* amplitude ratios. *P* wave polarities (solid symbols: compressions; open symbols: dilatations) and *P* wave nodes are shown in upper focal hemisphere equal area projection. From *Ross et al.* [1996].

magma and supercritical water. An alternative mechanism, proposed by *Ekström* [1994a], is shear slip on a ring fault [paper 1, section 4.2.2]. For a fault dipping at 75°, the strike would have to vary by 180° or more, whereas for a less steep fault, such as a cone-sheet, the range could be smaller.

Bardarbunga volcano, beneath the Vatnajökull ice cap in Iceland, generated six non-DC earthquakes of M_W 5.2–5.6 (M_0 = 8–30 × 10^{16} N m) between 1977 and 1993 [*Ekström*, 1994a]. According to the Harvard CMT catalog, they had nearly vertical CLVD-like mechanisms with ε values between 0.36 and 0.48 (Figure 11) that resemble those expected for ring faulting. For a dip of 75°, the observed ε values require that the strikes must span a range of 180°–250°. For faults dipping less than 55° the required range is less than 180°. Ring faults exposed in ancient calderas are usually vertical or dip steeply outward [e.g., *Clough et al.*, 1909] and are inefficient generators of non-DC earthquakes. Cone sheets, which dip (inward) less steeply, have more favorable geometry.

3.4. Earthquakes at Mines

Deep mine excavations strongly perturb the stresses in the surrounding rocks, reducing some components from values initially of the order of 100 MPa to practically zero. The resulting stress differences can exceed the strength of competent rocks and cause earthquakes (often called "rock bursts," "coal bumps," etc.). The seismic data available are often of superb quality, recorded on many multicomponent instruments and involving short propagation paths through homogeneous rock, free from the effects of weathering that degrade surface observations. Studies of such data show clearly that many earthquakes at mines have non-DC mechanisms, usually with predominantly dilatational first motions that are incompatible with orthogonal nodal planes [e.g., *Kusznir et al.*, 1984; *Rudajev and Sileny*, 1985; *Wong et al.*, 1989; *Wong and McGarr*, 1990].

An M_L 3.5 earthquake on May 14, 1981, at the Gentry Mountain mining region, Utah, had unusually small surface waves with spectra similar to those of explosions in the area [*Taylor*, 1994]. Surface wave amplitudes and initial phases require a volume decrease [*Patton and Zandt*, 1991]. This event coincided with the collapse of a large room at 200-m depth in the Gentry Mountain mine.

Stickney and Sprenke [1993] recorded 21 earthquakes on a 15-station network (Figure 12) at the Coeur d'Alene mining district, Idaho, and found that 90% of the *P* wave polarities were dilatational. Ten events had polarity distributions inconsistent with DC mechanisms.

The excavation of a 3.5-m-wide tunnel in unfractured,

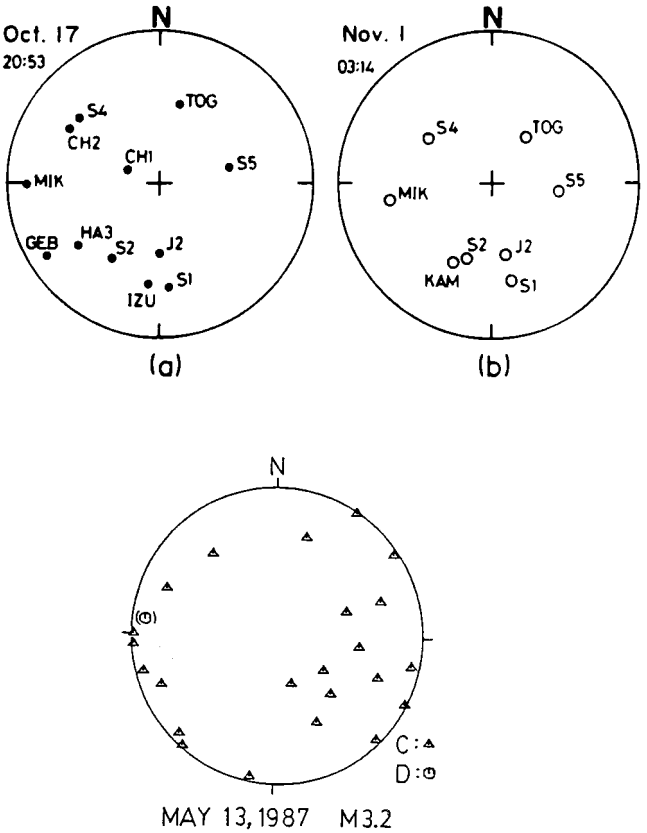

Figure 9. *P* wave polarities for three non-DC earthquakes at volcanic regions in Japan (upper focal hemispheres in equal area projection). (a, b) Earthquakes at Miyakejima Island in 1983 [*Shimizu et al.*, 1987]. Solid circles denote compressions; open circles indicate dilatations. (c) Earthquake of 13 May 1987 in the Unzen volcanic region (H. Shimizu, unpublished manuscript, 1987). Triangles denote compressions; circles indicate dilatations.

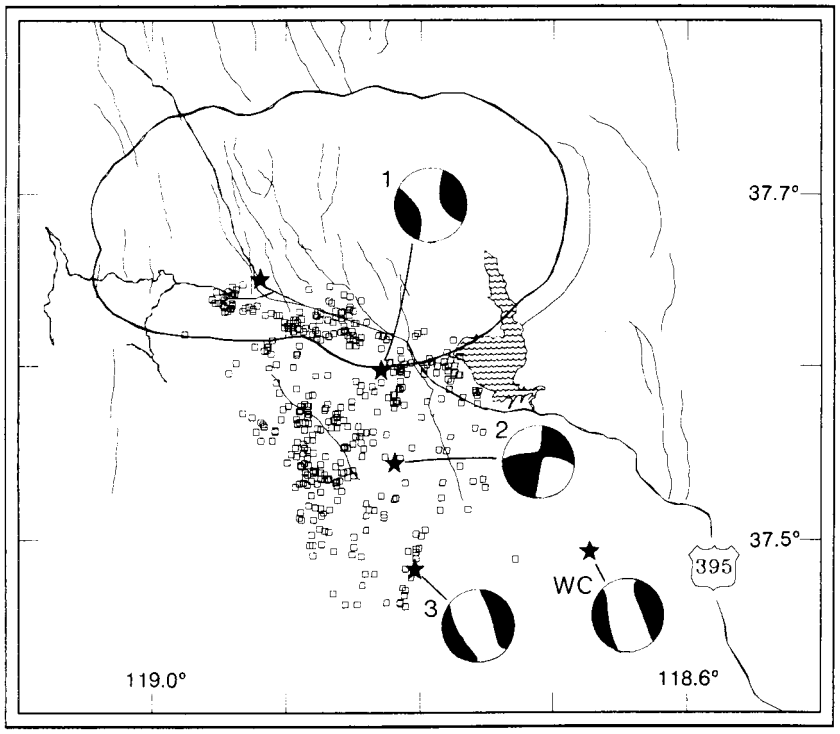

Figure 10. Long Valley caldera, California, and vicinity, showing best located earthquakes in 1980 with coda duration magnitude >3 and mechanisms for largest earthquakes of 1978 and 1980. (lower hemisphere equal area projections, with fields of compressional *P* wave polarity shaded). Labeled stars are as follows: WC, M_S 5.3 Wheeler Crest earthquake of October 4, 1978; 1, M_S 6.1 earthquake of 1634 UTC on May 25, 1980; 2, M_S 6.0 earthquake of 1945 on May 25, 1980; and 3, M_S 6.0 earthquake of 1451 on May 27, 1980. The unlabelled star marks the $M_S \geq 6$ earthquake of 1649 on May 25, 1980, whose mechanism cannot be determined well. The Wheeler Crest earthquake and earthquakes 1 and 3 have mechanisms with large non-DC components. The heavy line shows the caldera boundary. From *Julian and Sipkin* [1985]; Wheeler Crest earthquake mechanism from *Ekström and Dziewonski* [1983].

homogeneous granite at the Underground Research Laboratory (URL) in Manitoba, Canada, caused many non-DC earthquakes [*Feignier and Young*, 1992]. The tunnel was surrounded by 16 triaxial accelerometers, and hypocenter locations could be determined within about 0.5 m. Moment tensors computed for 33 earthquakes in the moment magnitude range −2 to −4 included tensile, implosive, and shear mechanisms. The 12 tensile events occurred near an area of breakout on the tunnel roof, whereas most of the six implosive earthquakes occurred ahead of the active face.

Brawn [1989] used a maximum entropy method to compute higher-rank moment tensors [paper 1, section 2.3.2) for four mining-induced earthquakes at a depth of 2.2 km in Westdriefontein, South Africa. Three of the mechanisms indicated shear failure preceded by a high-frequency, short-duration initiation phase. The fourth earthquake, located within 5 m of an active tunnel, had a mechanism that implied two different modes of failure on the same plane, oriented normal to the tunnel. The proposed process involves shear slip along a preexisting fracture, which simultaneously propagated into intact rock by tensile failure.

McGarr [1992a, b] inverted the polarities and amplitudes of near- and far-field *P* and *S* waves [paper 1, sections 3.2.3 and 3.3] (Figure 13) to determine moment tensors for 10 earthquakes within 150 m of deep gold mines in the Witwatersrand, South Africa. Seven of the events involved large volume decreases, with all principal moments negative and the most negative moments oriented approximately vertically. These events resemble the "implosive" earthquakes of *Feignier and Young* [1992].

3.5. Other Shallow Earthquakes

Unlike the planar idealizations used in mathematical analysis, real fault surfaces are rough, so "shear" slip must involve some motion normal to faults. Furthermore, motion occurs normal to even planar faults in laboratory experiments on stick-slip sliding in foam rubber [paper 1, section 4.3.4]. Kinematically, fault-normal motion is equivalent to tensile faulting. There is some evidence that such motion occurs in many earthquakes.

Haskell [1964] found that $P:S$ amplitude ratios at high frequencies are usually larger than those expected for shear faulting, and suggested that this indicates fault-normal motion caused by fault roughness. High $P:S$ amplitude ratios might also be caused by anelastic attenuation or *S*-to-*P* mode conversion, but the observed effect is too large to be explained entirely by propagation effects. The theoretical $P:S$ energy ratio for fault-normal motion is about 10 times greater than for shear faulting, so a small amount of fault-normal motion could explain the observed ratios.

High $P:S$ amplitude ratios at frequencies above 10 Hz were measured for local earthquakes at the Guerrero accelerometer array, Mexico [*Castro et al.*, 1991]. The ratio varies greatly for different source-station pairs but on average is far higher than expected for a DC source. The observations cannot be explained by attenuation effects alone and must be at least partly due to a source effect.

If two or more shear-faulting earthquakes occur nearly simultaneously, or if the fault orientation or slip direction changes as faulting proceeds, the overall mechanism of the event can have a non-DC component [paper 1, section 4.2.1], although some practically important

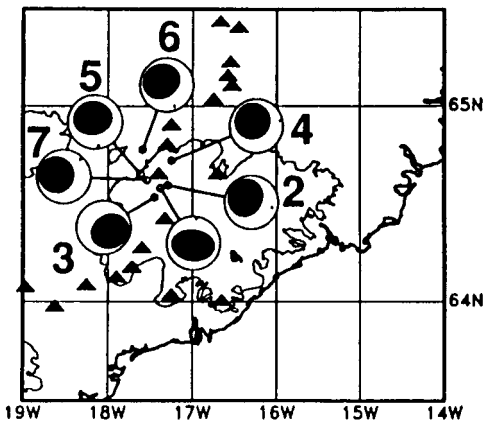

Figure 11. Map showing Harvard CMT mechanisms of earthquakes at Bardarbunga volcano, southeast Iceland, from *Ekström* [1994a]. Also shown are the southeast coast of Iceland and the outline of the Vatnajökull ice cap.

cases, such as conjugate faulting, give DC composite mechanisms. The moment tensor for such an earthquake can, however, never have a volumetric component.

Sipkin [1986a], in a study of the M_L 6.5 Coalinga, California, earthquake of May 2, 1983, found that constraining the moment tensor components to have similar time functions leads to a spurious non-DC result. If this constraint is removed, the derived moment tensor varies significantly with time and corresponds to a DC that rotates slightly during rupture propagation. The 1988 M_S 6.8 Armenian earthquake, which has an ε value of −0.20 in the Harvard CMT catalog, appears to result from multiple shear faulting also. The teleseismic body waveforms are complex for an event of this size, and aftershock locations suggest variations in fault orientation. Detailed moment tensor analysis using broadband and long-period records resolved three strike-slip DC subevents of approximately equal size in the first 20 s of rupture [*Pacheco et al.*, 1989]. Analysis of a longer interval suggests that an additional dip-slip event occurred about 30 s after the initial rupture [*Kikuchi et al.*, 1993]. The sum of these four separate DC mechanisms is similar to the non-DC Harvard CMT solution.

Large, normal-faulting MOR earthquakes recorded teleseismically often have *P* wave polarity distributions with reduced dilatational fields and nonorthogonal nodal surfaces [e.g., *Sykes*, 1967]. These are, however, probably artifacts of near-source wave propagation effects. Because MOR earthquakes are very shallow, the direct (*P*) and surface-reflected (*pP* and *sP*) phases arrive nearly simultaneously, and interference between

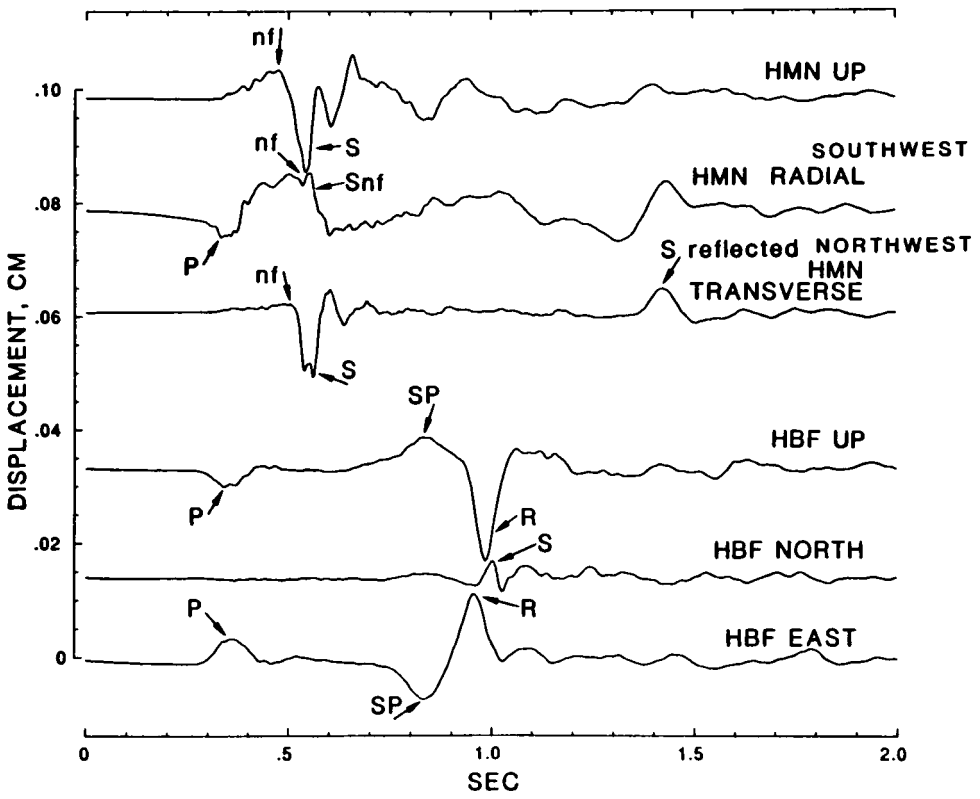

Figure 13. Displacement seismograms (doubly integrated accelerograms) from sites HMN (underground), and HBF (surface), for a non-DC earthquake at a deep gold mine in the Witwatersrand, South Africa. The phases *P*, near-field (nf), *S*-to-*P* conversion (*SP*), *S*, and surface-reflected *S* (*R*) are shown. The *P* phase and the near-field motion have opposite polarities on the radial component at HMN, implying that the source has an isotropic component. From *McGarr* [1992b, Figure 2]; copyright Birkhäuser Verlag AG, Basel, Switzerland.

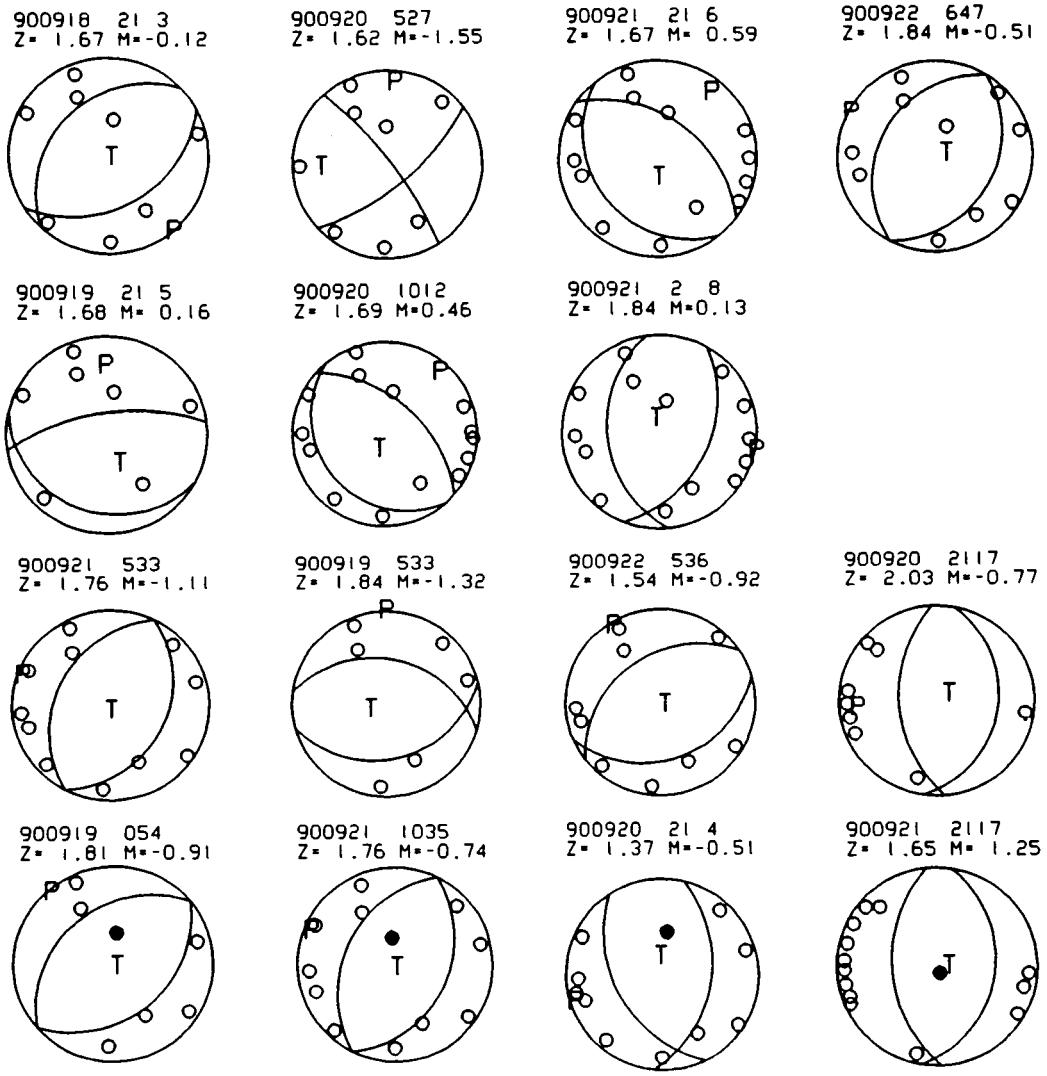

Figure 12. Earthquakes with predominantly dilatational *P* wave polarities from the Coeur d'Alene mining district, northern Idaho. Solid circles indicate compressional polarities; open circles show dilatations. Upper focal hemispheres are shown in equal area projection. From *Stickney and Sprenke* [1993].

them can reverse the apparent polarities for certain takeoff angles [*Hart*, 1978; *Trehu et al*., 1981]. In apparent disagreement with this, the moment tensors of large MOR earthquakes in the Harvard CMT catalog have systematically positive ε values averaging 0.057. These mechanisms are consistent with combined normal and strike-slip faulting [*Kawakatsu*, 1991a]. Such combinations can explain 70% of the well-constrained non-DC moment tensors for earthquakes in the Harvard catalog from "well-behaved" MOR segments, i.e., those located away from continental margins [*Frohlich*, 1995].

A well-recorded *Ms* 7.8 non-DC earthquake occurred at a depth of 28 km near Taiwan on November 14, 1986 [*Zheng et al*., 1995]. The earthquake was well recorded on 16 digital stations at regional and teleseismic distances and had *P* wave polarities inconsistent with shear faulting. Inversion of *P* and *SH* waveforms yielded a moment tensor equivalent to a reverse-slip DC combined with an implosion (Figure 2).

A similar but smaller (magnitude 4.6) earthquake on February 10, 1987 beneath the Kanto district, Japan, had dilatational *P* wave polarities over most of the focal sphere (Figure 14) [*Hurukawa and Imoto*, 1993]. The polarities are consistent with conical nodal planes with an apex angle of about 78°, implying an implosive isotropic component (the apex angle for a CLVD is 109.47°). This earthquake occurred within the subducting Philippine Sea plate at 57-km depth.

3.6. Deep-Focus Earthquakes

Both the frequency of earthquake occurrence and the rate of moment release have bimodal depth distributions, decreasing with depth to about 350 km and increasing below that. Deep earthquakes occur only beneath subduction zones. The minimum in activity at intermediate depths was once attributed to changes from tension to compression within descending lithospheric slabs, but extensive data on earthquake focal

mechanisms now contradict this hypothesis [*Green and Houston*, 1995]. The deep earthquake region coincides with the "transition zone" of the upper mantle, where polymorphic phase transformations in olivine produce two rapid increases in seismic wave speeds (the 400- and 670-km "discontinuities"). Earthquakes cease near 680 km, the base of the transition zone, even though there is evidence that slabs may penetrate deeper.

Phenomenologically, deep earthquakes differ in several respects from shallow ones. They produce fewer aftershocks, have shorter rise times and durations for events of the same magnitude [*Vidale and Houston*, 1993], they have more symmetrical source time functions (intermediate and shallow earthquakes tend to have moment release concentrated in the early portion of the source-time function) [*Houston and Vidale*, 1994]. The largest deep earthquakes tend to occur in regions that are otherwise relatively inactive. There is usually no obvious spatial relationship between a deep earthquake and its aftershocks [*Frohlich and Willemann*, 1987; *Willemann and Frohlich*, 1987], and neither aftershocks nor subevents cluster preferentially along the nodal planes of main shocks, although hypocenters of smaller earthquakes (not aftershocks) near major earthquakes are sometimes aligned [*Giardini and Woodhouse*, 1984; *Lungren and Giardini*, 1992]. All these facts suggest that deep and shallow earthquakes involve different physical processes.

The physical cause of deep earthquakes has posed an enigma since they were first recognized in the 1920s. Stick-slip frictional instability is inhibited by pressure, and plastic flow in minerals is enhanced by temperature, so stick-slip is not expected to occur below about 30 km in normal areas. Unusual conditions such as low temperature or high pore fluid pressure might extend this limit to 100 km or so in subduction zones, but not to the depths of almost 700 km to which earthquakes persist. Some other kind of instability must cause deep earthquakes. Processes that have been considered include plastic instabilities, shear-induced melting, and polymorphic phase transformation [*Green and Houston*, 1995]. A recently recognized variant of the last process, "transformational faulting" [paper 1, section 4.6], has dominated recent experimental and theoretical work on deep earthquakes.

The cessation of seismicity at the bottom of the upper-mantle transition zone near 680 km suggests that deep earthquakes may involve polymorphic phase transformations, but no experiments have yet convincingly resolved volume changes in their focal mechanisms. *Benioff* [1963] noted a resemblance between a strain seismogram recorded at Naña, Peru, from the $M_0 = 7 \times 10^{20}$ N m (M_W 7.9) Peru-Bolivia earthquake of August 15, 1963, and the theoretical prediction for an isotropic implosion, and speculated that the earthquake was caused by a rapid phase change, but it turns out that theoretical seismograms for other mechanisms are similar. One of the earliest moment tensor inversions of seismic data, applied to normal modes of the Earth [*Gilbert and Dziewonski*, 1975], gave large precursory volume changes about 100 s before the same 1963 Peru-Bolivia earthquake and the $M_0 = 2 \times 10^{21}$ N m (M_W 8.2) Colombian earthquake of July 31, 1970, but these may have been artifacts of laterally inhomogeneous structure [*Okal and Geller*, 1979]. Studies of more recent large earthquakes, based on more numerous and higher-quality data, have not detected volume changes. For example, high-quality observations of the $M_0 = 3 \times 10^{21}$ N m (M_W 8.3) Bolivian deep earthquake of June 9, 1994, show no evidence of a substantial volumetric component [*Hara et al.*, 1994; *Ekström*, 1994b]. *Kawakatsu* [1991b] analyzed long-period body waveforms of 19 deep earthquakes and found that their volumetric components are statistically unresolvable (<10% of the seismic moment). *Stimpson and Pearce* [1987] inverted *P*, *pP*, and *sP* amplitude ratios [paper 1, section 3.4] to determine moment tensors for three deep earthquakes in the Sea of Okhotsk in a search for volume changes, but found no evidence of them.

Deep earthquakes do, however, have systematically large non-DC components, even though they do not involve large volume changes. In other words, deep earthquakes have larger CLVD components than shallow ones (Figure 15). The size of CLVD components may increase systematically with depth and with event magnitude [*Houston*, 1993], but these conclusions are uncertain. *Kubas and Sipkin* [1987] reported a strong positive correlation between CLVD components and magnitudes for deep earthquakes in the Nazca Plate subduction zone but could not find a similar relationship elsewhere. The CLVD components of deep earthquake moment tensors determined using different inversion schemes and data sets often agree well [*Kuge and Kawakatsu*, 1993], which suggests that these components are not artifacts of particular methods.

Non-DC components of deep-focus earthquakes may be partially artifacts of unmodeled path effects. Subduction zones, where deep earthquakes occur, have higher seismic wave speeds than the surrounding mantle, because they are cooler than and compositionally different from it. Numerical simulation of the effects of a high-velocity slab on seismic waves shows that spurious non-DC components can be introduced into derived mechanisms if wavelengths are smaller than the slab thickness [*Tada and Shimazaki*, 1994].

The lack of large-volume changes in deep earthquakes is compatible with complex shear faulting [paper 1, section 4.2], and detailed waveform analysis resolves some deep non-DC earthquakes into DC subevents. For example, a deep earthquake that occurred January 1, 1984, south of Honshu has two prominent *P*-wave arrivals, consistent with DC sources of different orientations [*Kuge and Kawakatsu*, 1990, 1992]. Commonly, the DC subevents share a principal *P* or *T* axis that lies within the dipping slab [*Kuge and Kawakatsu*, 1993]. Eighty percent of the deep earthquakes in the Harvard CMT

catalog that have large non-DC components and small standard errors are consistent with pairs of DC earthquakes with particular orientations thought to be realistic (caused, for example, by downdip compression and slab bending) [*Frohlich*, 1995].

Glennon and Chen [1995] used *P* and *SH* waveforms to model the mechanisms of eight deep earthquakes in the northwestern Pacific, six of which showed evidence of rupture propagation, usually on subhorizontal planes. For most events the estimated rupture fits within the predicted thickness of the metastable olivine wedge.

The $M_0 = 3 \times 10^{21}$ N m (M_W 8.3) Bolivian earthquake of June 9, 1994, is the largest deep earthquake yet observed and provides the best data available from a deep earthquake. It occurred at a depth of 636 km in a region of the Nazca plate subduction zone characterized by anomalous deep seismicity [*Okal et al*., 1994]. Independent analyses of body and surface waves give similar mechanisms, corresponding to slip on a nearly horizontal, 40 to 50-km-long fault [e.g., *Kikuchi and Kanamori*, 1994; *Silver et al*., 1995], with no significant volume change [*Hara et al*., 1994; *Wu et al*., 1995; *Lundgren and Giardini*, 1995; *Ekström*, 1994b]. The inferred source dimensions greatly exceed the theoretical thickness of the hypothesized wedge of metastable olivine at 630 km (<10 km). Thus the fault must extend outside the cold core of the subducting slab. The earthquake had relatively few aftershocks, but they were close to the inferred mainshock rupture plane. Some aftershocks occurred outside the hypothesized metastable wedge. This earthquake inspired several new proposals for deep earthquake mechanisms [*Houston and Vidale*, 1994]. The earthquake rupture may have begun as transformational faulting within the metastable wedge and then extended out of it, possibly facilitated by shear melting (H. Kanamori, personal communication, 1995).

3.7. Non-DC Earthquakes in Moment Tensor Catalogs

Moment tensors for large earthquakes are now computed routinely [paper 1, section 3.5.3]. The Harvard CMT catalog is the most complete, containing over 11,000 events that occurred between 1978 and 1994 [e.g., *Dziewonski et al*., 1987]. Of these, hundreds of events have large and statistically significant non-DC components. These events occur in all tectonic environments and geographic areas [*Frohlich*, 1995].

There can be large discrepancies between the non-DC components for the same earthquake in the Harvard and U.S. Geological Survey (USGS) catalogs (Figure 16), with $|\varepsilon|$ values from the USGS catalog systematically smaller than those from the Harvard catalog [*Sipkin*, 1986b]. Different data are used for the two catalogs [paper 1, section 3.5.3], so some differences in the results are to be expected. Comparison of the two catalogs gives information on their reliabilities, and indicates that uncertainties are larger than the formal statistical estimates.

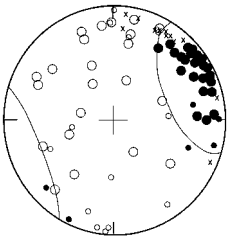

Figure 14. *P* wave polarities for the magnitude 4.6 non-DC earthquake of February 10, 1987 in the Kanto district, Japan. Nodal surfaces shown are for a "conical type" mechanism with an apex angle of 78°, which has both implosive isotropic and CLVD components. Open circles indicate dilatational polarities; solid circles show compressions. Different symbol sizes indicate data from different networks. The upper focal hemisphere is shown in equal area projection. From *Hurukawa and Imoto* [1993; Figure 5b].

There is an inverse correlation between ε and scalar moment for shallow thrust-faulting earthquakes in the Harvard catalog [*Kuge and Lay*, 1994b], but surface waves are used only for events with moments larger than about 10^{18} N m [*Dziewonski and Woodhouse*, 1983], so this correlation may be an artifact of the inversion process. It may also reflect the effect of noisy seismograms. For realistic station distributions and for certain DC source mechanisms, the addition of random noise with a standard deviation of 10% to seismograms can produced $|\varepsilon|$ values as large as 0.3 [*Satake*, 1985]. The most reliable non-DC moment tensors are those that are reproducible using different methods and different data sets, such as that of the Tori Shima earthquake (section 3.3) and some deep earthquakes (section 3.6) [*Kuge and Kawakatsu*, 1993].

4. DISCUSSION

The negative term "non-double-couple" is uninformative, expressing merely what an earthquake is not, and implying that it deviates from some standard. The observations now available make it clear that the term actually encompasses several physical phenomena, although our understanding of them is still highly incomplete. Furthermore, theoretical considerations and recent laboratory experiments hint that such processes may be intrinsic in the nucleation and continuation of predominately shear earthquakes also. Attention to non-DC processes is likely to become increasingly important as the quality of seismic data, the power of analytical methods, and the sophistication of our understanding of earthquake processes continue to increase.

Even earthquakes that are primarily due to shear faulting have small non-DC components, because of departures from ideal geometry such as fault curvature and roughness, and variations in slip direction. Furthermore, the formation of shear faults is thought to involve tensile microcracking, though this has not yet been detected by seismological methods.

Some kinds of events, such as landslides and volcanic

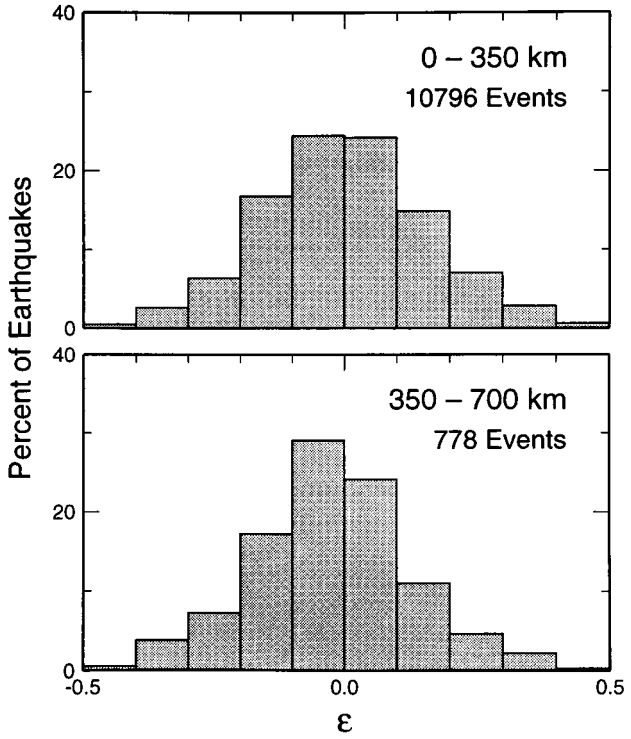

Figure 15. Observed distributions of ε, which measures the relative moments of CLVD components, for shallow and deep earthquakes in the Harvard CMT catalog between January 1, 1977, and May 31, 1994. Deep earthquakes have systematically more negative values.

eruptions, involve advection and require source representations more general than moment tensors, including net forces (section 3.1). In theory, landslides require net torques also, although no analyses to date have included these. Doing so might help to resolve inconsistencies such as that between seismological and field observations for the Mantato, Peru landslide.

A disproportionate fraction of non-DC earthquakes occur in volcanic and geothermal areas. Some, such as the Tori Shima earthquake, the Barbarbunga earthquakes, and the Long Valley earthquakes (section 3.3), have mechanisms close to pure CLVDs and may be caused by rapid intrusions, probably of gas-rich magma, although ring faulting or simultaneous slip on multiple shear faults is also possible. Other earthquakes in volcanic and geothermal areas (section 3.3) and mines (section 3.4) have mechanisms with isotropic components, involving volume increases or decreases. These are often consistent with mixed-mode failure involving simultaneous shear and tensile faulting. In geothermal areas, high-temperature/pressure geothermal fluids may enable tensile cracks to form and remain open at depths of several kilometers. At mines, tunnels may act as cavities that can close seismically. Data from MORs are not yet adequate to determine whether small, non-DC earthquakes occur there also, although the resemblance of geologic processes and structures at MORs to those in Iceland makes this likely. Some volcanic earthquake mechanisms include net forces (section 3.2), indicating that these events involve the advection of magmatic fluids. Analyses of volcanic earthquake mechanisms must allow for possible net force components if the source processes are to be fully understood.

Stick-slip sliding instability cannot operate beneath about 300 km depth. This fact, and various empirical seismological differences, suggest that deep and shallow focus earthquakes involve different physical processes. Moreover, seismic data indicate that deep focus earthquakes do not involve significant volume changes, even though they occur within the transition zone, a region of polymorphic phase transformations in the upper mantle. They do, however, have larger CLVD components, on average, than shallow earthquakes. Mechanisms of this type are consistent with simultaneous shear slip on differently oriented faults. Current theory attributes deep earthquakes to "transformational shear faulting," facilitated by phase changes in small "anticracks" in the same way that formation of ordinary shear faults is facilitated by tensile microcracks. It is not yet clear, however, why anticracks should favor simultaneous shear faulting.

ACKNOWLEDGMENTS. We thank Larry Ruff, David Hill, and two anonymous reviewers for critically reading the manuscript and suggesting improvements. This research was supported by a G. K. Gilbert Fellowship from the U.S. Geological Survey, NERC grant GR9/134, a Nuffield fellowship held by G.R.F., and a NERC Ph.D. studentship held by A.D.M.

Jim Smith was the Editor responsible for this paper. He thanks Larry Ruff and two anonymous referees for their reviews.

REFERENCES

Aki, K., Evidence for magma intrusion during the Mammoth Lakes earthquakes of May 1980 and implications of the absence of volcanic (harmonic) tremor, *J. Geophys. Res.*, *89*, 7689–7696, 1984.

Ando, M., The Hawaii earthquake of November 29, 1975: Low dip angle faulting due to forceful injection of magma, *J. Geophys. Res.*, *84*, 7616–7626, 1979.

Arnott, S. K., and G. R. Foulger, The Krafla spreading segment, Iceland, 1, Three-dimensional crustal structure and the spatial and temporal distribution of local earthquakes, *J. Geophys. Res.*, *99*, 23,801–23,825, 1994a.

Arnott, S. K. and G. R. Foulger, The Krafla spreading segment, Iceland, 2, The accretionary stress cycle and nonshear earthquake focal mechanisms, *J. Geophys. Res.*, *99*, 23,827–23,842, 1994b.

Barker, J. S., and C. A. Langston, A teleseismic body wave analysis of the May, 1980, Mammoth Lakes, California, earthquakes, *Bull. Seismol. Soc. Am.*, *73*, 419–434, 1983.

Benioff, H., Source wave forms of three earthquakes, *Bull. Seismol. Soc. Am.*, *53*, 893–903, 1963.

Brawn, D. R., A maximum entropy approach to underconstraint and inconsistency in the seismic source inverse problem; Finding and interpreting seismic source moments,

Ph.D thesis, 163 pp., Univ. of the Witwatersrand, Johannesburg, 1989.
Castro, R. R., J. G. Anderson, and J. N. Brune, Origin of high *P*/*S* spectral ratios from the Guerrero accelerograph array, *Bull. Seismol. Soc. Am.*, *81*, 2268–2288, 1991.
Clough, C. T., H. B. Maufe, and E. B. Bailey, The cauldron-subsidence of Glen Coe, and the associated igneous phenomena, *Q. J. Geol. Soc. London*, *65*, 611–678, 1909.
Doxsee, W. W., The Grand Banks earthquake of November 18, 1929, *Publ. Dom. Observ. Ottawa*, *7*, 323–335, 1948.
Dziewonski, A. M., and J. H. Woodhouse, An experiment in the systematic study of global seismicity: Centroid-moment tensor solutions for 201 moderate and large earthquakes of 1981, *J. Geophys. Res.*, *88*, 3247–3271, 1983.
Dziewonski, A. M., G. Ekström, J. E. Franzen, and J. H Woodhouse, Centroid-moment tensor solutions for January–March 1986, *Phys. Earth. Planet. Inter.*, *45*, 1–10, 1987.
Eissler, H. K., and H. Kanamori, A single-force model for the 1975 Kalapana, Hawaii, earthquake, *J. Geophys. Res.*, *92*, 4827–4836, 1987.
Ekström, G., Anomalous earthquakes on volcano ring-fault structures, *Earth Planet. Sci. Lett.*, *128*, 707–712, 1994a.
Ekström, G., Teleseismic analysis of the great 1994 Bolivia earthquake (abstract), *Eos Trans. AGU*, *75*(44), Fall Meet. Suppl., 465, 1994b.
Ekström, G. and A. M. Dziewonski, Moment tensor solutions of Mammoth Lakes earthquakes (abstract), *Eos Trans. AGU*, *64*, 262, 1983.
Ekström, G., and A. M. Dziewonski, Centroid-moment Tensor solutions for 35 earthquakes in western North America (1977 to 1983), *Bull. Seismol. Soc. Am.*, *75*, 23–39, 1985.
Feignier, B., and R. P. Young, Moment tensor inversion of induced microseismic events: Evidence of non-shear failures in the $-4 < M < -2$ moment magnitude range, *Geophys. Res. Lett.*, *19*, 1503–1506, 1992.
Foulger, G. R., Hengill Triple Junction, SW Iceland, 1, Tectonic structure and the spatial and temporal distribution of local earthquakes, *J. Geophys. Res.*, *93*, 13,493–13,506, 1988a.
Foulger, G. R., Hengill Triple Junction, SW Iceland, 2, Anomalous earthquake focal mechanisms and implications for processes within the geothermal reservoir at accretionary plate boundaries, *J. Geophys. Res.*, *93*, 13,507–13,523, 1988b.
Foulger, G. R., and B. R. Julian, Non-double-couple earthquakes at the Hengill-Grensdalur Volcanic Complex, Iceland: Are they the artifacts of crustal heterogeneity?, *Bull. Seismol. Soc. Am.*, *83*, 38–52, 1993.
Foulger, G. R., and R. E. Long, Anomalous focal mechanisms: Tensile crack formation on an accreting plate boundary, *Nature*, *310*, 43–45, 1984.
Foulger, G. R., R. E. Long, P. Einarsson, and A. Björnsson, Implosive earthquakes at the active accretionary plate boundary in northern Iceland, *Nature*, *337*, 640–642, 1989.
Frohlich, C., Earthquakes with non-double-couple mechanisms, *Science*, *264*, 804–809, 1994.
Frohlich, C., Characteristics of well-determined non-double-couple earthquakes in the Harvard CMT catalog, *Phys. Earth Planet. Inter.*, *91*, 213–228, 1995.
Frohlich, C., and R. J. Willemann, Aftershocks of deep earthquakes do not occur preferentially on nodal planes of focal mechanisms, *Nature*, *329*, 41–42, 1987.
Giardini, D., and J. H. Woodhouse, Deep seismicity and modes of deformation in the Tonga subduction zone, *Nature*, *307*, 505–509, 1984.
Gilbert, F., and A. M. Dziewonski, An application of normal mode theory to the retrieval of structural parameters and source mechanisms from seismic spectra, *Philos. Trans. R. Soc. London*, *Ser. A*, *278*, 187–269, 1975.

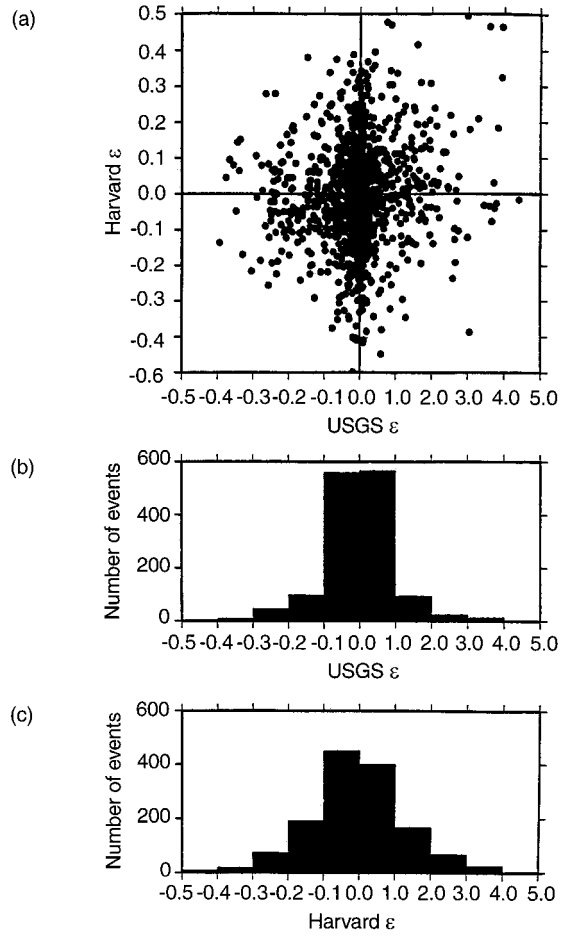

Figure 16. Comparison of the non-DC components of earthquakes in the Harvard CMT catalog and the USGS moment tensor catalog. (a) Values of ε for 1418 events between January 1980 and May 1994 that are in both catalogs. (b, c) Histograms of ε for the same data set. There is considerable disagreement between the ε values in the two catalogs.

Given, J. W., T. C. Wallace, and H. Kanamori, Teleseismic analysis of the 1980 Mammoth Lakes earthquake sequence, *Bull. Seismol. Soc. Am.*, *72*, 1093–1109, 1982.
Glennon, M. A., and W.-P. Chen, Ruptures of deep-focus earthquakes in the north-western Pacific and their implications on seismogenesis, *Geophys. J. Int.*, *120*, 706–720, 1995.
Green, H. W., III, and H. Houston, The mechanics of deep earthquakes, *Annu. Rev. Earth Planet. Sci.*, *23*, 169–213, 1995.
Hara, T., K. Kuge, and H. Kawakatsu, The determination of moment tensor of the 1994 Bolivia deep earthquake using various datasets of seismic waves at very broadband frequency (abstract), *Eos Trans. AGU*, *75*(44), Fall Meet. Suppl., 465, 1994.
Hart, R. S., Body wave studies of the September 1969 North Atlantic Ridge earthquake (abstract), *Eos Trans. AGU*, *59*, 1135, 1978.
Hasegawa, H. S., and H. Kanamori, Source mechanism of the magnitude 7.2 Grand Banks earthquake of November 1929: Double couple or submarine landslide?, *Bull. Seismol. Soc. Am.*, *77*, 1984–2004, 1987.
Hasegawa, A., D. Zhao, S. Hori, A. Yamamoto, and S. Horiuchi, Deep structure of the northeastern Japan arc and its relationship to seismic and volcanic activity, *Nature*, *352*, 683–689, 1991.

Haskell, N. A., Total energy and energy spectral density of elastic wave radiation from propagating faults, *Bull. Seismol. Soc. Am.*, *54*, 1811–1841, 1964.

Houston, H., The non-double-couple component of deep earthquakes and the width of the seismogenic zone, *Geophys. Res. Lett.*, *20*, 1687–1690, 1993.

Houston, H., and J. Vidale, The temporal distribution of seismic radiation during deep earthquake rupture, *Science*, *265*, 771–774, 1994.

Hurukawa, N., and M. Imoto, A non double-couple earthquake in a subducting oceanic crust of the Philippine Sea plate, *J. Phys. Earth*, *41*, 257–269, 1993.

Iguchi, M., A vertical expansion source model for mechanisms of earthquakes originating in the magma conduit of an andesitic volcano, Japan, *Bull. Volcanol. Soc. Jpn.*, *39*, 49–67, 1994.

Ishihara, K., Dynamical analysis of volcanic explosion, *J. Geodyn.*, *3*, 327–349, 1985.

Julian, B. R., Evidence for dyke intrusion earthquake mechanisms near Long Valley Caldera, California, *Nature*, *303*, 323–325, 1983.

Julian, B. R., and S. A. Sipkin, Earthquake processes in the Long Valley Caldera area, California, *J. Geophys. Res.*, *90*, 11,155–11,169, 1985.

Julian, B. R., A. D. Miller, and G. R. Foulger, Non-double-couple earthquake mechanisms at the Hengill-Grensdalur volcanic complex, southwest Iceland, *Geophys. Res. Lett.*, *24*, 743–746, 1997.

Julian, B. R., A. D. Miller, and G. R. Foulger, Non-double-couple earthquakes, 1, Theory, *Rev. Geophys.*, this issue.

Kanamori, H., and J. W. Given, Analysis of long period seismic waves excited by the May 18, 1980, eruption of Mt. St. Helens—A terrestrial monopole?, *J. Geophys. Res.*, *87*, 5422–5432, 1982.

Kanamori, H, J. W. Given, and T. Lay, Analysis of seismic body waves excited by the Mount St. Helens eruption of May 1980, *J. Geophys. Res.*, *89*, 1856–1866, 1984.

Kanamori, H., G. Ekström, A. Dziewonski, J. S. Barker, and S. A. Sipkin, Seismic radiation by magma injection—An anomalous seismic event near Tori Shima, Japan, *J. Geophys. Res.*, *98*, 6511–6522, 1993.

Kawakatsu, H., Centroid single force inversion of seismic waves generated by landslides, *J. Geophys. Res.*, *94*, 12,363–12,374, 1989.

Kawakatsu, H., Enigma of earthquakes at ridge-transform fault plate boundaries. Distribution of non-double couple parameter of Harvard CMT solutions, *Geophys. Res. Lett.*, *18*, 1103–1106, 1991a.

Kawakatsu, H., Insignificant isotropic component in the moment tensor of deep earthquakes, *Nature*, *351*, 50–53, 1991b.

Kikuchi, H., and H. Kanamori, The mechanism of the deep Bolivia earthquake of June 9, 1994, *Geophys. Res. Lett.*, *21*, 2341–2344, 1994.

Kikuchi, M., H. Kanamori, and K. Satake, Source complexity of the 1988 Armenian earthquake: Evidence for a slow after-slip event, *J. Geophys. Res.*, *98*, 15,797–15,808, 1993.

Klein, F. W., P. Einarsson, and M. Wyss, The Reykjanes Peninsula, Iceland, earthquake swarm of September 1972 and its tectonic significance, *J. Geophys. Res.*, *82*, 865–887, 1977.

Kubas, A., and S. A. Sipkin, Non-double-couple earthquake mechanisms in the Nazca plate subduction zone, *Geophys. Res. Lett.*, *14*, 339–342, 1987.

Kuge, K., and H. Kawakatsu, Analysis of a deep non-DC earthquake using very broad band data, *Geophys. Res. Lett.*, *17*, 227–230, 1990.

Kuge, K., and H. Kawakatsu, Deep and intermediate depth non-double couple earthquakes—Interpretation of moment tensor inversions using various passbands of very broadband seismic waves, *Geophys. J. Int.*, *111*, 589–606, 1992.

Kuge, K., and H. Kawakatsu, Significance of non-double couple components of deep and intermediate earthquakes—Implications from moment tensor inversions of long period seismic waves, *Phys. Earth. Planet. Inter.*, *75*, 243–266, 1993.

Kuge, K., and T. Lay, Data-dependent non-double-couple components of shallow earthquake source mechanisms: Effects of waveform inversion instability, *Geophys. Res. Lett.*, *21*, 9–12, 1994.

Kusznir, N. J., N. H. Al-Singh, and D. P. Ashwin, Induced-seismicity generated by longwall coal mining in the North Staffordshire coal field, U.K., in *Rockbursts and Seismicity in Mines*, *S. Afr. Inst. Min. Metall. Symp. Ser.*, no. 6, edited by N. C. Gay and E. H. Wainwright, pp. 153–160, 1984.

Lundgren, P. R., and D. Giardini, Seismicity, shear failure and modes of deformation in deep subduction zones, *Phys. Earth. Planet. Inter.*, *74*, 63–74, 1992.

Lundgren, P., and D. Giardini, The June 9 Bolivia and March 9 Fiji deep earthquakes of 1994, I, Source processes, *Geophys. Res. Lett.*, *22*, 2241–2244, 1995.

McGarr, A., An implosive component in the seismic moment tensor of a mining-induced tremor, *Geophys. Res. Lett.*, *19*, 1579–1582, 1992a.

McGarr, A., Moment tensors of 10 Witwatersrand mine tremors, *Pure Appl. Geophys.*, *139*, 781–800, 1992b.

Miller, A. D., Seismic structure and earthquake focal mechanisms of the Hengill volcanic complex, SW Iceland, Ph.D. thesis, 280 pp., Univ. of Durham, 1996.

Okal, E. A., and R. J. Geller, On the observability of isotropic sources: the July 31, 1970, Colombian earthquake, *Phys. Earth Planet. Inter.*, *18*, 176–196, 1979.

Okal, E. A., E. R. Engdahl, S. H. Kirby, and W.-C. Huang, Deep South American earthquakes: the general context of the large 09 June 94 Bolivia shock, an extraordinary event in an extraordinary Wadati-Benioff Zone (abstract), *Eos Trans. AGU*, *75*, 465, 1994.

Pacheco, J. F., C. H. Estabrook, D. W. Simpson, and J. L. Nabelek, Teleseismic body wave analysis of the 1988 Armenian earthquake, *Geophys. Res. Lett.*, *16*, 1425–1428, 1989.

Patton, H. J., and G. Zandt, Seismic moment tensors of western U.S. Earthquakes and implications for the tectonic stress field, *J. Geophys. Res.*, *96*, 18,245–18,259, 1991.

Ross, A., G. R. Foulger, and B. R. Julian, Non-double-couple earthquake mechanisms at the Geysers geothermal area, California, *Geophys. Res. Lett.*, *23*, 877–880, 1996.

Rudajev, V., and J. Sileny, Seismic events with non-shear components, II, Rockbursts with implosive source component, *Pure Appl. Geophys.*, *123*, 17–25, 1985.

Rundle, J. B. and D. P. Hill, The geophysics of a restless caldera—Long Valley, California, *Annu. Rev. Earth Planet. Sci.*, *16*, 251–271, 1988.

Satake, K., Effects of station coverage on moment tensor inversion, *Bull. Seismol. Soc. Am.*, *75*, 1657–1667, 1985.

Satake, K. and H. Kanamori, Abnormal tsunamis caused by the June 13, 1984, Tori Shima, Japan, earthquake, *J. Geophys. Res.*, *96*, 19,933–19,939, 1991.

Shimizu, H., S. Ueki, and J. Koyama, A tensile-shear crack model for the mechanism of volcanic earthquakes, *Tectonophysics*, *144*, 287–300, 1987.

Shimizu, H., N. Matsuwo, and S. Ohmi, A non double-couple seismic source: Tensile-shear crack formation in the Unzen Volcanic Region, *Seismol. Res. Lett.*, *59*, 5, 1988.

Silver, P. G., S. L. Beck, T. C. Wallace, C. Meade, S. C. Meyers, D. E. James, and R. Kuehnel, Rupture characteristics of the deep Bolivian earthquake of 9 June 1994 and the mechanism of deep-focus earthquakes, *Science*, *268*, 69–73, 1995.

Sipkin, S. A., Interpretation of non-double couple earthquake

mechanisms derived from moment tensor inversion, *J. Geophys. Res*., *91*, 531–547, 1986.
Sipkin, S. A., Estimation of earthquake source parameters by the inversion of waveform data: Global seismicity 1981–1983, *Bull. Seismol. Soc. Am*., *76*, 1519–1541, 1986b.
Stickney, M. C., and K. F. Sprenke, Seismic events with implosional focal mechanisms in the Couer d'Alene mining district, northern Idaho, *J. Geophys. Res*., *98*, 6523–6528, 1993.
Stimpson, I. G., and R. G. Pearce, Moment tensors and source processes of three deep Sea of Okhotsk earthquakes, *Phys. Earth. Planet. Inter*., *47*, 107–124, 1987.
Sykes, L. R., Mechanism of earthquakes and nature of faulting on the mid-oceanic ridges, *J. Geophys. Res*., *72*, 2131–2153, 1967.
Tada, T. and K. Shimazaki, How much does a high-velocity slab contribute to the apparent non-double-couple components in deep-focus earthquakes?, *Bull. Seismol. Soc. Am*., *84*, 1272–1278, 1994.
Taylor, S. R., False alarms and mine seismicity: An example from the Gentry Mountain mining region, Utah, *Bull. Seismol. Soc. Am*., *84*, 350–358, 1994.
Toomey, D. R., S. C. Solomon, G. M. Purdy, and M. H. Murray, Microearthquakes beneath the median valley of the Mid-Atlantic Ridge near 23°N: Hypocenters and focal mechanisms, *J. Geophys. Res*., *90*, 5443–5458, 1985.
Toomey, D. R., S. C. Solomon, and G. M. Purdy, Microearthquakes beneath the median valley of the Mid-Atlantic Ridge near 23°N: Tomography and tectonics, *J. Geophys. Res*., *93*, 9093–9112, 1988.
Trehu, A. M., J. L. Nabelek, and S. C. Solomon, Source characterization of two Reykjanes Ridge earthquakes: Surface waves and moment tensors, *P* waveforms, and nonorthogonal nodal planes, *J. Geophys. Res*., *86*, 1701–1724, 1981.
Ueki, S., H. Shimizu, J. Comm, and A. Takagi, Seismic activity following the 1983 eruption of Miyakejima, in The 1983 eruption of Miyakejima, *Bull. Volcanol. Soc. Jpn*., *Ser. II*, *29*, S81–S100, 1984.
Uhira, K., and M. Takeo, The source of explosive eruptions of Sakurajima volcano, Japan, *J. Geophys. Res*., *99*, 17,775–17,789, 1994.
Ukawa, M., and M. Ohtake, A monochromatic earthquake suggesting deep-seated magmatic activity beneath the Izu-Ooshima volcano, Japan, *J. Geophys. Res*., *92*, 12,649–12,663, 1987.
Vidale, J. E., and H. Houston, The depth dependence of earthquake duration and implications for rupture mechanisms, *Nature*, *365*, 45–47, 1993.
Willemann, R. J., and C. Frohlich, Spatial patterns of aftershocks of deep focus earthquakes, *J. Geophys. Res*., *92*, 13,927–13,943, 1987.
Wong, I. G., and A. McGarr, Implosional failure in mining-induced seismicity: A critical review, in *Rockbursts and Seismicity in Mines*, edited by C. Fairhurst, pp. 45–51, A. A. Balkema, Brookfield, Vt., 1990.
Wong, I. G. J. R. Humphrey, J. A. Adams, and W. J. Silva, Observations of mine seismicity in the eastern Wasatch Plateau, Utah, U.S.A.: A possible case of implosional failure, *Pure Appl. Geophys*., *129*, 369–405, 1989.
Wu, J., T. Wallace, and S. Beck, A very broadband study of the 1994 deep Bolivia earthquake sequence, *Geophys. Res. Lett*., *22*, 2237–2240, 1995.
Zheng, T., Z. Yao, and P. Liu, The 14 November 1986 Taiwan earthquake—an event with isotropic component, *Phys. Earth Planet. Inter*., *91*, 285–298, 1995.

G. R. Foulger and A. D. Miller, Department of Geological Sciences, University of Durham, Durham, DH1 3LE, England, U.K.

B. R. Julian, U.S. Geological Survey, 345 Middlefield Road, MS 977, Menlo Park, CA 94025. (e-mail: julian@andreas.wr.usgs.gov)